sciendo

Civil and Environmental Engineering
Vol. 19, Issue 1, 348-356, DOI: 10.2478/cee-2023-0031

REINFORCED CONCRETE BEAMS WITHOUT SHEAR REINFORCEMENT USING FIBER REINFORCED CONCRETE AND ALKALI-ACTIVATED MATERIAL

Radoslav GANDEL[1,*], Jan JERABEK[1], Zuzana MARCALIKOVA[1]

[1] Faculty of Civil Engineering, VSB-Technical University of Ostrava, Ludvíka Podéště 1875/17, 708 00 Ostrava-Poruba, Czech Republic.
[*] corresponding author: radoslav.gandel.st@vsb.cz

Abstract

Concrete, which is based on the use of Portland cement as a binder, often becomes a construction material in the construction industry. Concrete itself, however, exists in a number of modifications that are intended for specific applications. Especially with regard to the development of materials engineering, variants were created, which include, for example, fiber reinforced concrete with improved tensile properties and alkaline-activated composite, which produces less CO_2 emissions. The aim of the presented article is to verify the concept of using a combination of reinforced concrete and alkaline-activated material in the application of reinforced concrete beams without shear reinforcement. Components of the experimental program are static load tests, which are evaluated in detail with regard to the formation and propagation of cracks. Laboratory tests are also part of the experimental program, which focus on a detailed description of the properties and the possibility of a technological solution.

Keywords:

Reinforced concrete beam;
Fiber reinforced concrete;
Alkali-activated material;
Material properties;
Experiment.

1 Introduction

Concrete, which is based on the use of Portland cement [1] as a binder, often becomes a construction material in the construction industry in the past and the present. Concrete itself, however, exists in a number of modifications that are intended for specific applications [1]. Typically, this is, for example, high-strength concrete, high-performance concrete [2] or fiber reinforced concrete [3, 4] and many others. However, the production of cement has a high energy demand and represents a significant share of the total CO_2 emissions in the world [5]. The need for innovation of concrete recipes and careful use of raw materials was also stated within the framework of the sustainability principles of designing concrete structures according to the upcoming Model Code 2020 recommendation from the global organization fib for concrete [6]. The potential to replace cement with suitable substitutes [7], e.g. alkaline-activated systems, as stated by prof. Palomo [8], highlights raw materials created as by-products from industrial processes. Typically, these are blast furnace slag and power plant fly ash [9], which with the right additives and admixtures, due to their favorable hydraulic properties, can partially or completely replace the cement binder in concrete [10]. The actuality of the need to use secondary raw materials as part of the partial replacement of Portland cements can also be demonstrated by the development of low-carbon cements, when cements of the CEM I category will gradually be limited in production [11]. Possible solutions include the use of hybrid cements [12]. The research and testing of alkaline activated materials [13-16] itself has been going on for several decades, but its use in practice is still at an early stage. Frequent limitations of experimental programs include that they only focus on one selected property or description, and the characterization of the materials used is insufficient for wider generalization [13-16].

Interesting variants of concrete include fiber reinforced concrete [17-19]. The mentioned variant of concrete tries to improve mainly the tensile strength characteristics. Fiber reinforced concrete itself exists in a whole range of variants, where the fibers can differ in shape, material and termination. The mechanical properties are particularly affected by the dosage, which is typically up to 2 percent.

Numerical modeling is also often used to identify parameters [20]. Interesting application possibilities include, in particular, slabs interacting with the subsoil [17, 19] and beams without shear reinforcement [4]. In these cases, the typical failure mechanism is shear or push through [21-24]. For the most part, it is possible to use the same standards for the tests of reinforced concrete and concrete, but there are certain specifics where, for example, fracture energy and residual tensile strength belong.

As part of the presented research, a research idea arose on how to use the advantageous properties of reinforced concrete and combine them with an alkaline-activated material, which is a certain alternative material to reduce the overall energy demand. Specifically, the problem is solved on reinforced concrete supports made of reinforced concrete, which, however, are lightened by the longitudinal opening. However, the negative consequences of the above-mentioned solution are a reduction in bending stiffness and the emergence of larger vertical deformations, which can be a key design criterion, e.g. lintels above a window, etc. For this reason, an alkali-activated composite is used as a filler. A hybrid composite reinforced concrete beam will be created, which is the subject of an experimental program. The given task is also specific with regard to the technological possibilities of using alkaline-activated material.

2 Experimental program

The main subject of the experimental laboratory tests in the presented work are lightweight reinforced concrete beams made of fiber reinforced concrete without shear reinforcement and the additionally reinforced variant of these beams. The loading must be carried out with minimal a negative effect on the test results, which is detailed describing by CSN 73 2030 [25].

The content of the testing in the experimental part is 4 lightweight reinforced concrete beams with a span of 900 mm and 1500 mm (and their additionally strengthened variant with alkaline activated material) with a load in the middle of the span and with a typical test configuration as in the three-point bending test. The scheme of the trapezoidal cross-section of the beams with the cover of the reinforcement and the size of the hole is show in Fig. 1, cross-sectional diagram of the beam in Fig. 2. The reinforcement cover was 25 mm for all beams.

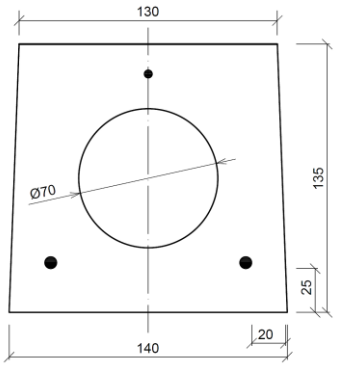

Fig. 1: Cross-section diagram of test beams.

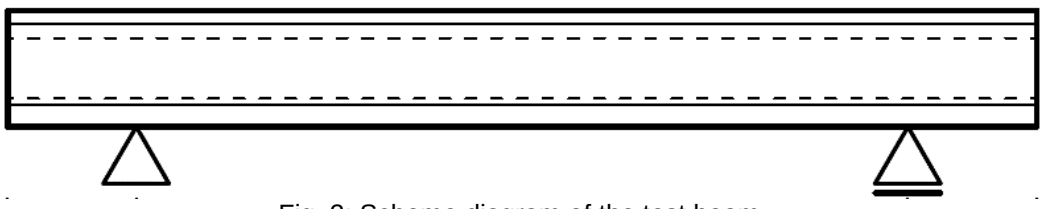

Fig. 2: Scheme diagram of the test beam.

Reinforcement rod with a diameter of 5 and 6 mm, depending on the span of the beam, is used, located longitudinally at the lower edge of the beams. At the upper edge, a reinforcement with a diameter of 4 mm is additionally used (with the exception of beams with a span of 900 mm), which eliminates possible deformations caused by handling the beams and which does not affect the observed properties. The fiber-reinforced concrete composite used belongs to the concrete class C30/37, with steel fibers with one end bend of length 40 mm and diameter 0.5 mm shown in Fig. 3. All information is shown in Table 1.

Fig. 3: Fibers.

Table 1: Information on test beams.

Designation	Type of beam	Length [mm]	Span [mm]	Reinforcement diameter [mm]
P1	Lightened	1190	900	5
P2		1190	900	5
P3		1790	1500	6
P4		1790	1500	6
V1	Additional reinforced	1190	900	5
V2		1190	900	5
V3		1790	1500	6
V4		1790	1500	6

Beams V1 - V4 with a span of 900 mm and 1500 mm were additionally strengthened with alkaline activated material with a binder based on blast furnace slag, see Fig. 4, with the formula per 1 m^3:

- Finely ground blast furnace slag Štramberk JMŠ 420: 450 kg,
- Water glass: 56.3 kg,
- Technical potassium hydroxide 50 %: 42 kg,
- Water: 172 l,
- Plasticizing additive Chrysoplast 760: 9 kg,
- Aggregate 0/4 Tovačov: 920 kg,
- Aggregate 4/8 Litice: 670 kg.

Fig. 4: Detail of the post-filled beam with alkali-activated material.

On the basis of laboratory tests, it was determined that the average compressive strength was 72 MPa and the bending tensile strength was 5.6 MPa. All mentioned beams were tested using a three-point bending test to verify the overall load-bearing capacity, cracks appearing in the area of the lower surface were identified on them and their detailed examination during the experimental test. In the images with the location of the cracks, the main flexural cracks are marked in red, minor flexural cracks in black.

For the proposed alkali-activated composite, specialized tests for fresh mixture and tests for hardened mixture are carried out. The test specimens are prisms meeting the requirements of the standard [26] ČSN EN 12390-1: Testing of hardened concrete - Part 1: Shape, dimensions and other requirements for test specimens and forms, placed on standard support rollers, located at a specified distance. The principle of loading is further different from the type of bending test. The three-point bending test consists of loading with one load roller in the center of the sample span at a speed of 0.04-0.06 MPa/s until the sample breaks. Fig. 5 illustrates the issue of bending tests.

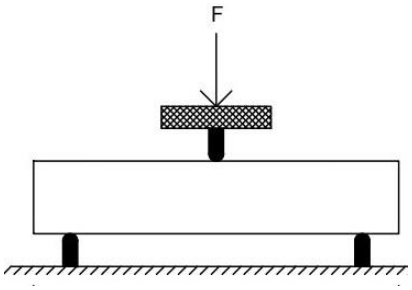

Fig. 5: Scheme of three-point bending test.

3 Results of reinforced beams

3.1 Results of beams with a support span of 900 mm

The first series of tested structural elements were beams with a support span of 900 mm. The scale diagram of the beams together with the location of the cracks is shown in Fig. 6. Beams P1 and P2 represent lightweight reinforced concrete beams made of fiber reinforced concrete, beams V1 and V2 their additionally strengthened variant with alkali-activated material. The test of beam with a support span of 900 mm is shown in Fig. 7.

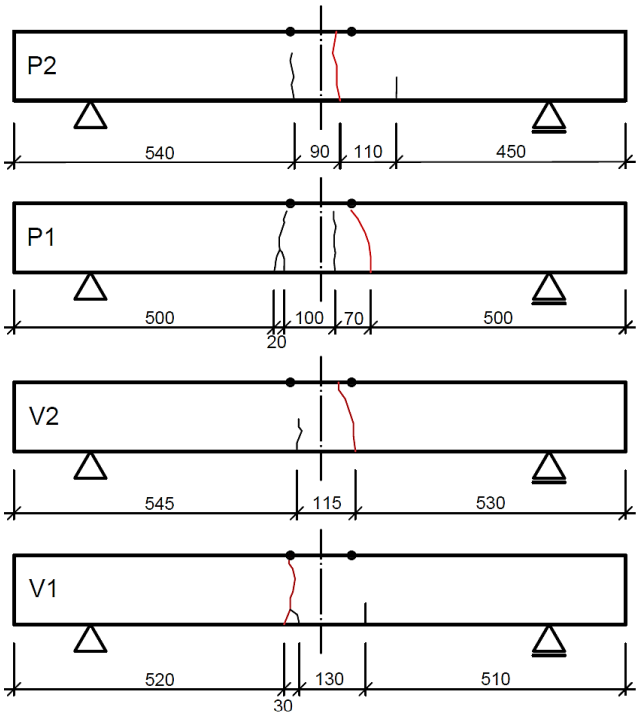

Fig. 6: Location of cracks on beams P1, P2, V1 and V2.

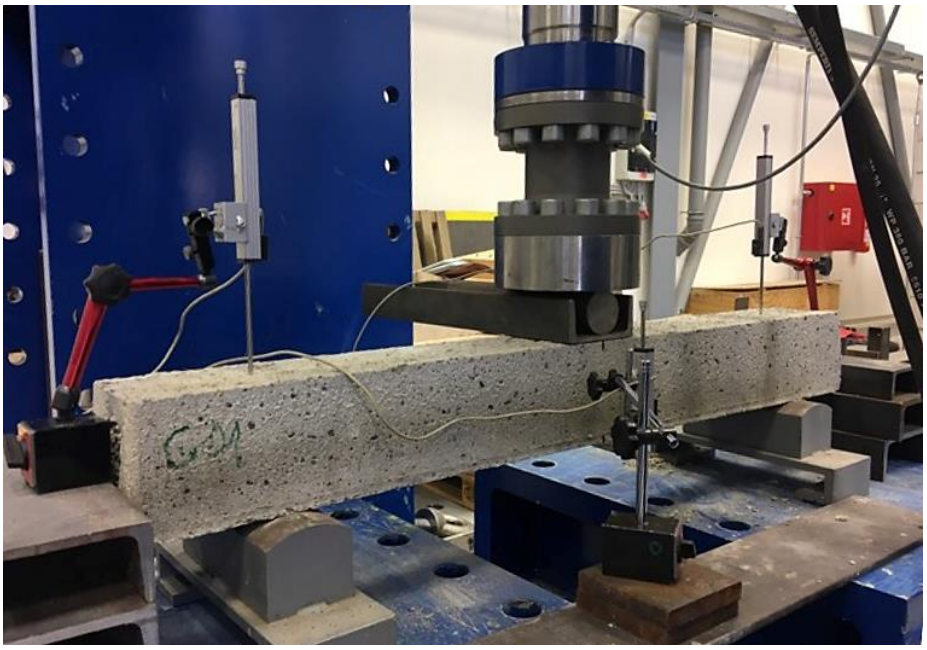

Fig. 7: The static load test on a beam with a support span of 900 mm.

Beams P1 and P2 shown in the graph in Fig. 8 represent a light version of the beams. Beams V1 and V2 their additionally reinforced alternative. The beams were loaded using an increase in deformation.

The first crack on beam P1 appeared in the third loading state, with a prescribed transverse deformation of 2 mm, with a width of 0.05 mm. In the next loading step, at a deformation of 2.5 mm, four cracks with a width of up to 0.05 mm appeared, which arose under a load of 13.74 kN. The gradual development of cracks was also noted in the following loading steps. The major flexural crack widened to 0.2 mm under a load of 15.79 kN with a prescribed deformation of 6.5 mm. The maximum load in the last loading step was 16.3 kN. At this point, the crack reached a maximum width of 0.3 mm. After exceeding this limit, there was a gradual decrease in the load while the deformation grew, which eventually led to the collapse of the beam. The crack mesh can be seen in Fig. 6.

Beam P2 behaved in the same way as beam P1 in the loading state with a prescribed deformation of 2 mm – a crack with a width of 0.05 mm was formed. The development of cracks in the following load conditions was not significant. A clear failure development occurred at a load of 15.1 kN, which was achieved for a prescribed deformation of 6.5 mm. The width of the cracks at this point was 0.1 - 0.2 mm, maximum 0.3 mm. After this loading step, as in the case of beam P1, there was a decrease in load with an increase in deformation and its subsequent failure of bearing capacity.

The course of the deformation load for beams P1 and P2 was the same, the collapse also occurred in both beams in the deformation range of around 11 - 13 mm. The resulting course of the load curve is similar in both cases, but the maximum load achieved for beam P1 is 16.3 kN, while for beam P2 15.3 kN.

In the case of beams additionally strengthened with alkali-activated material based on slag binder with a span of 900 mm, the same loading procedure was chosen as for their lighter version. The first cracks on beam V1, with a width of 0.05 – 0.1 mm, started to appear again in the load step with a prescribed deformation of 2 mm. At a prescribed deformation of 3.5 mm, with an achieved load of approximately 15 kN, cracks developed to a width of 0.2 mm. When the maximum load of 16.0 kN was reached, the main flexural crack widened to 0.7 mm. As for beam V2, the first cracks started to appear at a load of 14.2 kN, with a width of up to 0.2 mm. With a prescribed deformation of 4.5 mm, a maximum load of 15.6 kN was achieved and a crack with a width of up to 1.4 mm developed. From this point on, there was already a decrease in load with an increase in deformation and the subsequent collapse of the beam.

In both cases of additionally strengthened beams, it is possible to observe a smaller incidence of bending cracks, see Fig. 6, beams V1 and V2, but the maximum crack width was larger compared to the lightened beams P1 and P2. From the graph in Fig. 8, it is possible to further deduce the contribution of the filling geopolymer to the overall stiffness of the beams.

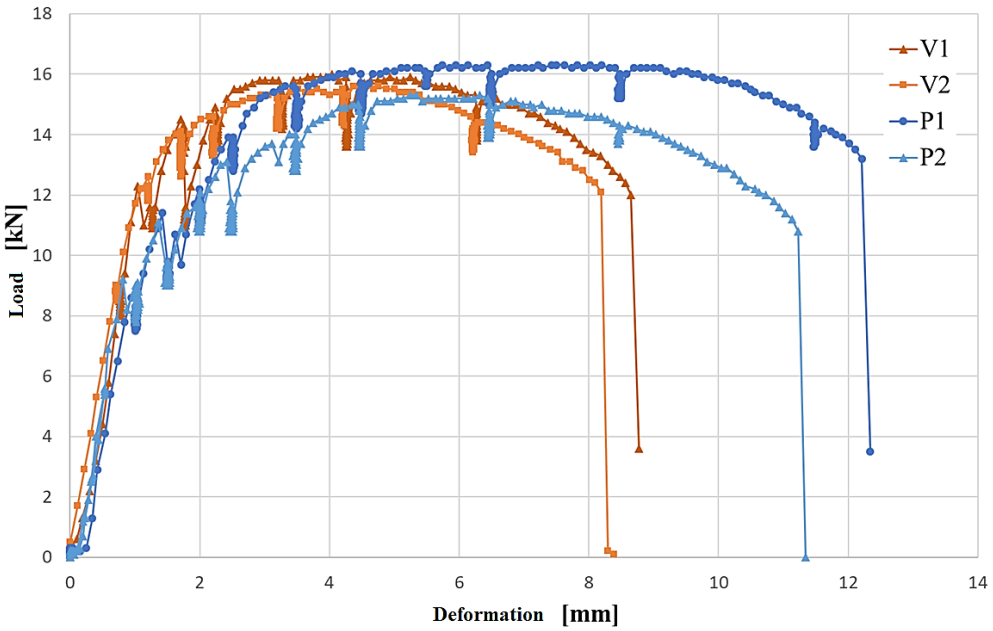

Fig. 8: Load-displacement diagram for beams V1, V2, P1 and P2.

3.2 Results of beams with a support span of 1500 mm

The second series of tested structural elements were beams with a support span of 1500 mm. Photo documentation of broken beams in Fig. 9. Again, in this case, both lightened reinforced concrete beams made of reinforced concrete P3, P4 and their additionally reinforced alternative V3, V4 were tested. The beams were loaded using an increase in deformation.

Fig. 9: Crack mesh on beams after collapse P3, P4, V3 and V4.

Reinforced concrete beams are shown in the graph in Fig. 10 marked P3 and P4. The first crack occurred on beam P3 during the third load step with a prescribed deformation of 3 mm and a width of 0.05 mm. In the next loading step, several cracks with a width of up to 0.1 mm appeared. The relevant load condition corresponded to the prescribed deformation of 4 mm. In the following loading conditions, the cracks developed gradually. With the prescribed deformation of 10 mm, the cracks reached a width of 0.2 - 0.3 mm. In addition, new cracks also appeared. The maximum load achieved for beam P3 was 12.5 kN. Just before the collapse of the beam, the maximum crack width of 0.5 mm was measured.

Beam P4 was also loaded using the same procedure. The first crack started to appear in the load step with a prescribed deformation of 3 mm, where it reached a width of approximately 0.1 - 0.15 mm. A marked difference could be observed at a load of 10.9 kN with a prescribed deformation of 8 mm. The cracks at this point reached 0.1 - 0.2 mm. The maximum crack width at the maximum load of 11.5 kN was 0.3 - 0.4 mm. In both cases, we can observe the resulting mesh of cracks in Fig. 9. The collapse of both beams occurred with deformations in the range of 18 - 30 mm.

With the additionally reinforced type of beams with a support span of 1500 m, marked in the graph in Fig. 10 V3 and V4, the same procedure was used as in the lighter version of the given beams. In the case of beam V3, the first crack appeared with a width of 0.05 mm at the prescribed deformation of 3 mm. At a load of 10.9 kN with a prescribed deformation of 3 mm, a crack developed up to 0.2 mm. The maximum load reached was 11.2 kN, while the maximum crack width in this case was up to 3.5 mm.

The development of cracks in the case of beam V4 was similar to that of beam V3. The first cracks started to appear at the prescribed deformation of 4 mm, with a width of up to 0.1 mm. The maximum load achieved on the V4 beam was 13.3 kN with a maximum width of up to 1.6 mm. From this moment, the load was reduced with an increase in deformation until the final collapse of the beam.

In both cases, we can claim that the additional strengthening in the form of alkali-activated material contributed to the bending stiffness of the beams, see graph in Fig. 10, and to the occurrence of fewer cracks, see Fig. 9, than in the case of lightened beams. On the contrary, wider cracks appeared in the additionally reinforced version of the beams.

The summary results of the experiment are shown in Table 2.

Table 2: Maximum load bearing capacities of test beams.

Beam	Load [kN]	Beam	Load [kN]
P1	16,3	V1	16,0
P2	15,3	V2	15,6
P3	12,5	V3	11,2
P4	11,5	V4	13,3

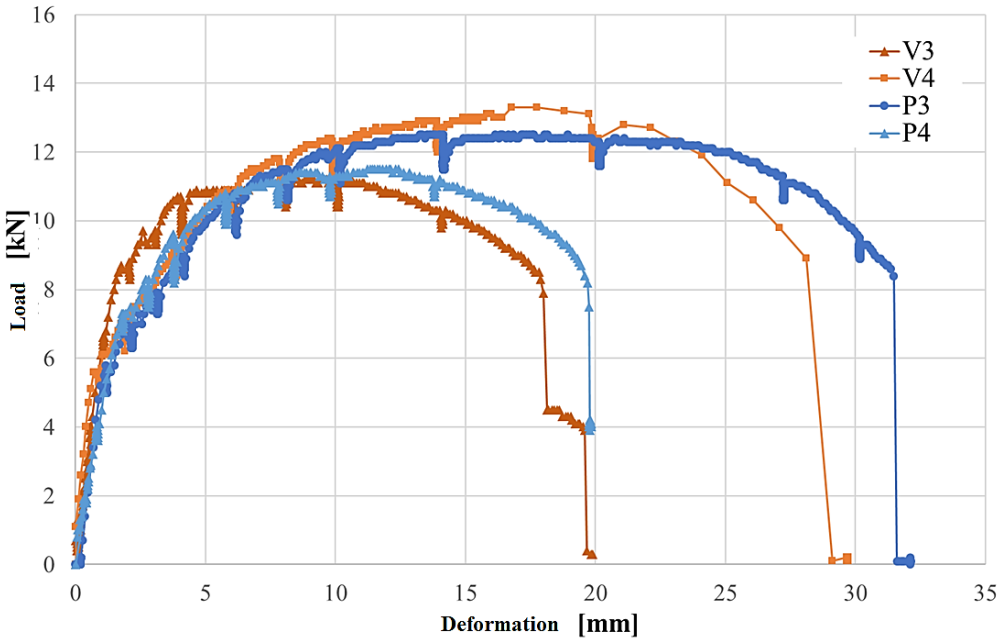

Fig.10: Load-displacement diagram for beams V3, V4, P3 and P4.

4 Conclusion

The purpose of the experimental part of the presented experimental program was focused on static load tests and the identification of cracks and their development on lightweight reinforced concrete beams made of fiber-reinforced concrete and on their additionally strengthened variant with an alternative and ecologically advantageous material.

The series of structural elements tested by static load tests included a light version of beams with a span of 900 and 1500 mm. The alternative group consisted of additionally reinforced beams with given spans. The material used for their additional reinforcement was a geopolymer based on a slag binder, whose main advantage is the use of secondary raw materials in its production, which reduces its financial costs and impact on the environment.

In the case of lightweight beams, the formation of several cracks with a relatively small width was typical. The resulting cracks were characteristic of bending stress. At a larger span, the resulting deformation for the maximum load reached more than 1/50 of the span. The development of flexural cracks initially occurred in the middle of the beam under the load at the lower surface, and with the increase in deformation, new cracks gradually appeared towards the supports.
Beams additionally strengthened with alkali-activated material showed an increase in bending stiffness compared to the lightened version. In addition, there was less occurrence of flexural cracks in these beams, but the width of these cracks was greater than that of the lightened beams. Additional strengthening with an ecological and economic material, as in the case of geopolymer based on slag binder, appears to be favorable, but considering the higher weight, the application of these beams is not suitable for constructions that emphasize this feature.

The negative of the geopolymer used (apart from the low impact on the environment) remains the rapid onset of solidification, which significantly limits the transport over longer distances and the subsequent handling of this mixture, which was also confirmed during the additional strengthening of the test beams. In the interests of sustainable development, the goal of future research is to further investigate and improve this building material with considerable potential.

The presented experimental program of lightweight reinforced concrete beams evaluated the experiments in detail. The use of reinforced concrete in combination with a light cross-section of reinforced concrete beams without shear reinforcement appears to be an effective solution. It is advantageous to further use the results of the experiment in the numerical modeling of their behavior [27].

Acknowledgement

This article has been achieved with the financial support of the Ministry of Education, specifically by the Student Research Grant Competition of the Technical University of Ostrava under identification number SP2023/058.

References

[1] COLLEPARDI, M.: The New Concrete. Grafiche Tintoretto, 2010, p. 436.
[2] MATECKOVA, P. - BILEK, V. - SUCHARDA, O.: Comparative study of high-performance concrete characteristics and loading test of pretensioned experimental beams. Crystals, 11 (4), 2021 art. No. 427.
[3] VAVRUS, M. – KRALOVANEC, J.: Study of Application of Fiber Reinforced Concrete in Anchorage Zone. Buildings, Vol. 13, Iss. 2, 2023, art. No. 524, doi: 10.3390/buildings13020524.
[4] SUCHARDA, O. - MARCALIKOVA, Z. - GANDEL, R.: Microstructure, Shrinkage, and Mechanical Properties of Concrete with Fibers and Experiments of Reinforced Concrete Beams without Shear Reinforcement. Materials, Vol. 15, 2022, 5707, https://doi.org/10.3390/ma15165707.
[5] Cement Carbon Dioxide Emissions Quietly Double in 20 Years, https://news.wttw.com/2022/06/22/cement-carbon-dioxide-emissionsquietly-double-20-years.
[6] HÁJEK, P.: Principles of sustainability in designing concrete structures according to MC2020. Proceedings of the Conference 28. Concrete Days, ČBS 2022 (in Czech).
[7] JUENGER, M. - WINNEFELD, F. - PROVIS, J. L. - IDEKER, J.: Advances in alternative cementitious binders. Cem. Concr. Res., Vol. 41, 2011, pp. 1232-1243.
[8] PALOMO, A. – GRUTZECK, M. W. – BLANCO, M. T.: Alkali-activated fly ashes: A cement for the future. Cement and Concrete Research, Vol. 29 (8), 1999, pp. 1323-1329.
[9] PROVIS, J. - VAN DEVENTER, J. S. J.: Eds. Alkali Acivated Materiále. State-of-Art-Report, Rilem TC 224-AAM, 2014.
[10] PROVIS, J.: Geopolymers and other alkali activated materials: Why, how, and what? Materials and Structures, Vol. 47 (1-2), 2014, pp. 11-25.
[11] GEMRICH, J. – VESELÝ, V.: Low carbon cements. Nízkouhlíkové cementy 2023, Sborník 18. konference Technologie a provádění 2023 (in Czech).
[12] PALOMO, A. - MONTEIRO, P. - MARTAUZ, P. - BILEK, V. - FERNANDEZ-JIMENEZ, A.: Hybrid binders: A journey from the past to a sustainable future (opus caementicium futurum). Cement and Concrete Research, Vol. 124, 2019, art. No. 105829, doi: 10.1016/j.cemconres.2019.105829.
[13] COLLINS, F. - SANJAYAN, J. G.: Workability and mechanical properties of alkali activated slag concrete, Cem. Donce. Res. Vol. 29, 1999, pp. 455-458.

[14] AMRAN, M. - FEDIUK, R. - MURALI, G. - AVUDAIAPPAN, S. - OZBAKKALOGLU, T. - VATIN, N. - KARELINA, M. - KLYUEV, S. - GHOLAMPOUR, A.: Fly Ash-Based Eco-Efficient Concretes: A Comprehensive Review of the Short-Term Properties. Materials, Vol. 14, 2021, 4264.
[15] MOHAMMED, A. A. - AHMED, H. U. - MOSAVI, A.: Survey of Mechanical Properties of Geopolymer Concrete: A Comprehensive Review and Data Analysis. Materials, Vol. 14, 2021, 4690.
[16] BILEK, V. - SUCHARDA, O. - BUJDOS, D. Frost Resistance of Alkali-Activated Concrete - An Important Pillar of Their Sustainability. Sustainability, Vol. 13, 473. https://doi.org/10.3390/su 13020473
[17] ALROUSAN, R. Z. - ALNEMRAWI, B. R.: The influence of concrete compressive strength on the punching shear capacity of reinforced concrete flat slabs under different opening configurations and loading conditions. Structures, Vol. 44, 2022, pp. 101-119, doi: 10.1016/j.istruc.2022.07.091
[18] KANG, S. T. - LEE, Y. - PARK, Y. D. - KIM, J. K.: Tensile fracture properties of an Ultra High Performance Fiber Reinforced Concrete (UHPFRC) with steel fiber. Composite Structures, Vol. 92 (1), 2010, pp. 61-71, doi: 10.1016/j.compstruct.2009.06.012.
[19] AZIZIAN, H. - LOTFOLLAHI-YAGHIN, M. A. – BEHRAVESH, A.: Punching Shear Strength of Voided Slabs on the Elastic Bases. Iranian Journal of Science and Technology - Transactions of Civil Engineering, Vol. 45 (4), 2021, pp. 2437 - 2449, doi: 10.1007/s40996-020-00546-y.
[20] SUCHARDA, O. - KONECNY, P. - KUBOSEK, J. - PONIKIEWSKI, T. - DONE, P.: Finite Element Modelling and Identification of the Material Properties of Fibre Concrete. Procedia Engineering, Vol. 109, 2015. pp. 234-239.
[21] HAITHAM, H. SAEED: Effect of Soil Nonlinearity on Analysis of Raft Foundation. Civil and Environmental Engineering, Vol. 18, Iss.1, 2022, pp. 292-300, doi: https://doi.org/10.2478/cee-2022-0027.
[22] HEGGER, J. - SHERIF, G. A. - RICKER, M.: Experimental investigations on punching behavior of reinforced concrete footings. ACI Structural Journal, Vol. 103, 2006, pp. 604–613.
[23] HALVONIK, J. - MAJTANOVA, L.: Experimental Investigation of the Maximum Punching Resistance of Slab-Column Connections. Slovak Journal of Civil Engineering, Vol. 26, 2018, pp. 22-28, doi:10.2478/sjce-2018-0017.
[24] TOMASOVICOVA, D. - JENDZELOVSKY, N. - MARTON, P.: Damage analysis of the industrial floor in the storage hall. International Multidisciplinary Scientific GeoConference Surveying Geology and Mining Ecology Management, SGEM, Vol. 17, Iss. 12, 2017, pp. 191-198, doi: 10.5593/sgem2017/12/S02.025.
[25] 73 2030 Static load tests of building structures. 5/2019.
[26] ČSN EN 12390-1: Testing hardened concrete – Part 1: Shape, dimensions and other requirements for specimens and moduls. 11/2021.
[27] SUCHARDA, O. - BROZOVSKY, J. - MIKOLASEK, D.: Numerical modelling and bearing capacity of reinforced concrete beams. Key Engineering Materials, Vol. 577-578, 2014, pp. 281-284.